Eddy Current System for Material Inspection and Flaw Visualization

R. BACHNAK, S. KING, W. MAEGER
Texas A&M University-Corpus Christi
Department of Computing Sciences
6300 Ocean Drive
Corpus Christi, Texas 78412, USA

T. NGUYEN
Johnson Space Center
Mail code ES4
2101 NASA Road 1
Houston, TX 77058-3696

Abstract: - Eddy current methods have been successfully used in a variety of non-destructive evaluation applications including detection of cracks, measurements of material thickness, determining metal thinning due to corrosion, measurements of coating thickness, determining electrical conductivity, identification of materials, and detection of corrosion in heat exchanger tubes. This paper describes the development of an eddy current prototype that combines positional and eddy-current data to produce a C-scan of tested material. The preliminary system consists of an eddy current probe, a position tracking mechanism, and basic data visualization capability. Initial test results of the prototype are presented in this paper.

Key-Words: eddy current, position tracking, visualization

1 Introduction

Nondestructive Testing (NDT) plays an important role in ensuring that components and systems are free of defects that compromise their functionality. NDT testing techniques, for example, are used to locate flaws that might otherwise cause major catastrophic events such as plane crashes, train accidents, and plant explosions. The tests are performed in such a way that objects under inspection are not damaged or affected in any way. Nondestructive Evaluation (NDE) refers to the process of locating defects and providing some measurements about the defect such as length, depth, and orientation. While there are several NDT methods, the three widely used techniques for materials testing and evaluation are radiography, ultrasonic, and eddy-current. In the case of eddy current, electrical currents are generated in a conductive material by an induced alternating magnetic field. Interruption in the flow of current due to imperfections or changes in the material's properties indicate some type of flaw. The eddy current method has been used in several industries, including space [1, 2] and chemical processing [3, 4]. Some specific applications include detection of cracks [5, 6, 7, 8, 9], measurements of material thickness [10], determining metal thinning due to corrosion [11], measurements of coating thickness [12], conversion coating [13], determining electrical conductivity [14], heat damage detection [3], and detection of corrosion in heat exchanger tubes [4]. This paper presents the development of an eddy current prototype that combines positional and eddy-current data to produce a visual representation of materials being tested. The system consists of an eddy current probe, a position tracking mechanism, and basic data visualization capability.

2 Eddy Current Technique

The eddy current method relies on the principle of magnetic induction using an alternating current. When an alternating current is supplied to the eddy current transducer (primary coil), an alternating magnetic field is produced. This

magnetic field induces a current in a second coil (pick up coil) in close proximity to it. Eddy currents flow in circles in the material being tested. An interruption in the flow of eddy currents may be directly linked to imperfections, such as cracks. In general, an eddy current system is used to inspect a relatively small area and the probe must be selected after a good understanding of the type of defect to be detected. Eddy current data can be collected manually or using automated scanning systems, where the probe moves at a constant speed. Automated systems have the advantage of minimizing changes in lift-off and accurate indexing due to the constant speed. Lift-off refers to the separation between the probe and the surface of the material being tested. Eddy current density decreases exponentially with depth as shown in Fig. 1.

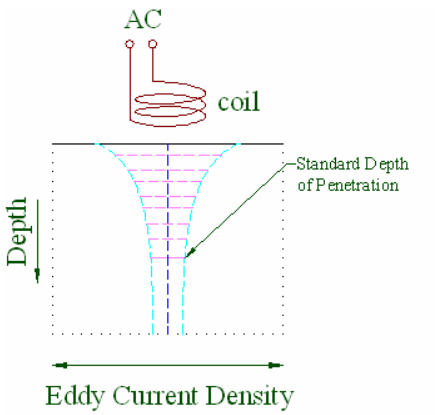

Figure 1. Eddy current density in function depth

The depth of the eddy currents is a function of the frequency of the excitation current and both the electrical conductivity and the magnetic permeability of the material. The depth of penetration decreases with increasing frequency and increasing conductivity and magnetic permeability. The depth at which eddy current density has decreased to 1/e, or about 37% of the surface density, is called the standard depth of penetration (δ) and is given by the following equation.

$$\delta = \frac{1}{\sqrt{\pi f \mu \sigma}} \qquad (1)$$

Where

δ = Standard Depth of Penetration (mm)
π = 3.14159
f = Test Frequency (Hz)
μ = Magnetic Permeability (H/mm)
σ = Electrical Conductivity (% IACS)

μ is equal to $\mu_r \mu_0$. μ_0, the permeability of free space, is equal to $4\pi \times 10^{-7}$ N/A. At two standard depths of penetration (2δ), the eddy current density decreases to 1/e squared or 13.5% of the surface density. At three depths (3δ), the eddy current density decreases to only 5% of the surface density.

The minimum thickness for a desired standard depth of penetration may be given by [15]:

$$\text{Minimum thickness} = 2.6 * \delta \qquad (2)$$

where δ is given by

$$\delta = 26 * (f \sigma)^{-1/2} \qquad (3)$$

This equation, compared to equation 1, assumes an aluminum material with a relative permeability μ_r of 1. Using equations 2 and 3, then the optimum frequency for a desired standard depth of penetration in aluminum is given by:

$$f = 676 * \delta^{-2} * \sigma^{-1} \qquad (4)$$

For surface cracks, the frequency should be as high as possible for increased resolution. For subsurface cracks, lower frequencies are required. Reference standards of similar material and thickness to the component being inspected and with representative defects should be available. These standards typically consist of three or four aluminum plates that are fastened together, with artificially induced cracks located in the different layers.

3 Position Tracking

Two devices were evaluated for the purpose of detecting positional data. The first device,

ShapeTape by Measurand Inc., is an array of fiber optic bend and twist sensors attached to a thin flexible substrate. Light intensity is used to calculate six-degree-of-freedom Cartesian data (x, y, z, roll, pitch, and yaw) at closely-spaced intervals along the tape. Test results showed that this device is not suitable for the proposed system. The second device is a laser computer mouse, MX-1000 by Logitech, consisting of the following three major components: (a) A low power laser with a fault protection circuit, (b) A lens that focuses the light emitted from the laser to illuminate the surface seen by the imaging chip, and (c) An imaging chip that contains a digital signal processor and an image acquisition system. The laser mouse was tested using a milling machine and AutoCAD. The laboratory setup is shown in Fig. 2, with the red arrow pointing to the mouse.

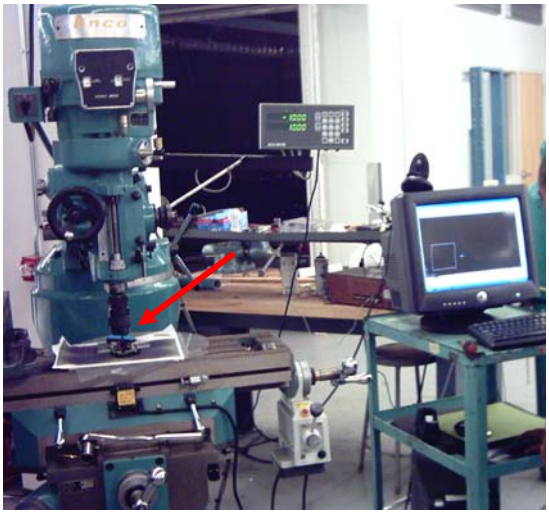

Figure 2. Laser mouse testing set up

The milling machine precisely controls the physical distances that the device moves while AutoCAD records the movements produced by the mouse and accurately dimensions them. A gradient pattern was created to provide an optimal surface for the laser mouse to determine its movements. This surface is used to minimize surface generated error so that only the error generated from the Charged Coupled Device (CCD) is recorded. It is also used to determine a scaling factor to adjust the scale within AutoCAD for the tests. The testing surface was raised to the device as close as possible. The sensing device must be in a perpendicular position in relation to the bottom of the test piece. AutoCAD was set for sketching using increments of 0.001. The sketch feature draws a series of attached straight lines in relation to the movement of the mouse. The increment size determines the length of the attached lines. The larger the increment sizes, the more jagged the curves will appear. The "pendown" command was used to cause AutoCAD to record the mouse movements. Scanning a square shape by moving 10 mm in each direction was used to produce a10x10 mm square. Once the square is completely drawn, it is scaled. This is needed as the sketch feature in AutoCAD draws the same sketch size in relation to screen size regardless of how far out you are zoomed. A scale factor is determined through the use of the average distance for all sides of the entire test performed on the gradient pattern. Recorded data is entered into Excel and the average for each direction is calculated as well as the standard deviation. Sample test results are shown in Table 1. Average % error varied between 1.5% and 7.6%

It is important to note that the mouse works by shining a light source, in this case a laser, at an angle onto the surface and using an imaging sensor to collect the bounced light. Using motion detection algorithms, relative motion of the mouse is determined. However, this motion is relative to the sensor chip. If the sensor chip is rotated, then the relative motion vectors also rotate. With a single mouse there is no way to detect this rotation.

Table 1. Sample test results, unit is mm

Test #	Up	Left to Right	Down	Right to Left	Start to End Offset Distance
1	10.47	9.54	10.33	10.48	0.37
2	10.28	9.21	11.42	9.54	0.33
3	9.29	9.02	10.47	9.06	1.03
4	9.72	9.68	10.85	9.63	1.03
5	9.62	9.58	9.62	8.78	0.71
6	9.43	9.02	10.76	9.35	1.18

4 Development of a Prototype

Fig. 3 shows the hardware used in the current prototype. The major components are an eddy current system, the Nortec 2000D+, an eddy current probe, a Copperhead laser mouse by Razer, and a data acquisition device, USB-1208FS. The USB-1208FS interfaces the Nortec 2000D+ with the laptop.

4.1 Acquiring Positional Data

To be able to produce a visualization of defects, positional data is combined with eddy current data to produce a C-scan of the examined material. To acquire positional data, an MX-1000 laser mouse was originally employed. This mouse has a 800DPI resolution and an update rate of 250Hz. To be able to detect a feature that is .050", then a sample is needed every .025". That means the probe can travel no faster than .025"*250/s = 6.25"/s. To scan the target surface of 12"x12" it would take about 1.92s for each scan. To detect features .050", a scan every, .025" would be required, or 480 scans, which would take a minimum of 15 ½ minutes. An improved mouse, the Razer Copperhead, has recently become available. The Copperhead images at 4000 DPI and has a refresh rate of 1000Hz. This increased resolution and 4x update rate, will decrease both the error and the scan time. The current system uses a cross-platform API, called ManyMouse, that abstracts using multiple mice into a single small library [16].

Figure 3. Prototype major components

4.2 Digitizing Data from the Probe

The Nortec 2000D+ eddy current system, the device used in the prototype, operates at 6000 Hz. Along with displaying the sensor information on its built-in screen, the Nortec 2000D+ also has two analog outputs that correspond to the horizontal and vertical positions of the cursor on the screen. These outputs must be digitized before they can be used. For testing purposes, a Measurement Computing USB-1208FS digitizer was used. This 12-bit digitizer has a USB interface which allows easy interface with the laptop. It also allows the display of information as it is captured on the laptop's screen.

The USB-1208FS digitizer is not designed to be a low-latency digitizer. That is, it cannot digitize samples at 6000 Hz. Since two signals have to be sampled, its effective capture rate is halved. However, since the positional data is only updated at 1000 Hz, the digitizer only needs a comparable speed. The USB-1208FS is giving around 150 Hz, which is adequate for testing purposes. The USB-1208FS can be put in continuous scan mode, or in single capture mode. In continuous scan mode, it captures multiple samples and returns them. In this mode it is capable of capturing at much higher rates, on the order of 100 KHz. However, in order to use the mode, a complex multithreading system that has a high-precision clock would be required. It is also possible to use a more expensive and faster digitizer. The final system will use a higher speed digitizer and will be repackaged with the position sensors.

The software library that comes with the USB-1208FS is binary-only, and only works on Windows XP. Currently, a Linux driver, written by Warren Jasper of NC State, is used [16]. This is the only piece of the system that is not platform independent. However, it is only an initialization routine, and a call to collect a sample that needs to be updated.

4.3 Testing the Prototype

The prototype was tested by using the mouse in conjunction with the eddy current probe to

create a visualization of the surface flaws on an aluminum plate. Fig. 4 shows the front side of an aluminum test plate. The plate is approximately .250" thick and has 8 grooves 1" apart. The grooves are rounded at the bottom and are .015" thick. The depths of the grooves are: .005", .010", .040", .060", .080", .100", .100", and .200". Since the grooves are rounded, the first groove isn't as thick as the others, but about .010" thick. Protective tape was applied to the plate to keep it from getting scratched by the probes. Fig. 5 shows a visualization of the front side of this test plate using a pencil probe operating at 300 KHz. The visualization was made with our system that determined position using a single Copperhead mouse and a USB-1208FS digitizer. The probe and mouse were held together as shown in Fig. 4. Since the mouse and probe were not held a fixed distance from each other, and since the mouse was held by hand there are positional errors. However, Fig. 5 demonstrates the feasibility of the system for detecting front-side cracks and shows that visualization with this approach is possible.

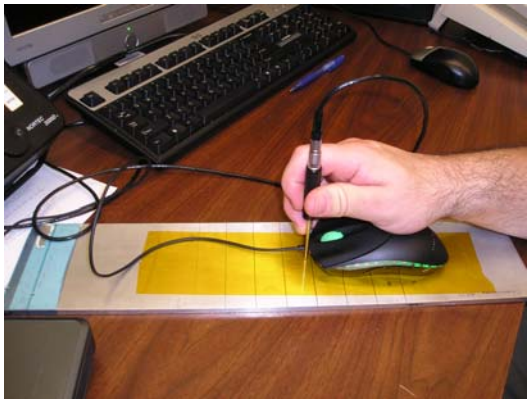

Figure 4. Scanning an aluminum plate

Visualizations were developed as C++ programs written for Linux. They use OpenGL [17] for performing the graphics. OpenGL is a cross-platform graphics library. All of the code for this project, except for the Linux-only USB-1208FS Linux driver, uses cross-platform libraries that have source code available. Even though C++ is used, there are few advanced features used, and with a small effort the entire project can be recompiled in C.

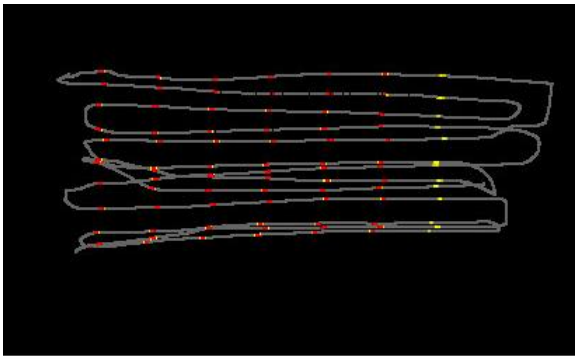

Figure 5. Visualization of plate shown in Fig. 4

The prototype was also tested for a backside inspection of the plate. The backside inspection was completed with a 100 Hz – 20 KHz frequency probe. Since the probe is much thicker then a pencil probe (0.6"), it responds to the same crack over a larger distance. This causes much larger lines in the visualization. Fig. 6 shows results of a sample test with an operational frequency of 300 Hz.

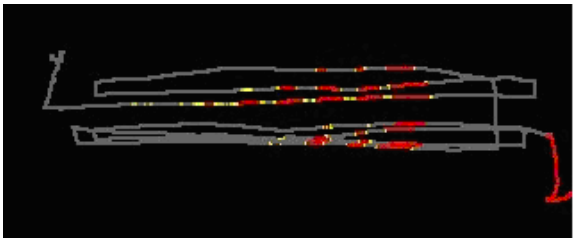

Figure 6. Visualization of a backside inspection

5 Conclusion

This paper describes the development of an eddy current prototype that combines positional and eddy-current data to produce a C-scan of tested material. The preliminary system consists of an eddy current probe, a position tracking mechanism, and basic data visualization capability. Preliminary test results support our belief that the system is feasible and practical.

Acknowledgement
This project is partially supported by grant from NASA-Johnson Space Center.

References:

[1] R. Smith, G. Hugo, "Transient Eddy-current NDE for Aging Aircraft – Capabilities and Limitations," Proc 4th Joint DoID/FAA/NASA Conf on Aging Aircraft, May 2000.

[2] A. Ahmed, J. G. Bakuckas, Jr., C. A. Bigelow, P. W. Tan, J. Awerbuch, A. Lau, and T. Tan, "Initiation and Distribution of Multiple-Site Damage (MSD) in a Fuselage Lap Joint Curved Panel," Proceedings of the 5th Joint NASA/FAA/DoD Conference on Aging Aircraft, September 10-13, 2001, Kissimmee, FL.

[3] A. Birring and G. Marshall, "Eddy Current Testing in the Petrochemical Industry," Materials Evaluation, November 2003.

[4] Helle H. Rasmussen, Hans Kristensen, and Leif Jeppesen, "NDT and Heat Exchanger Tubes," NDT.net October 1998, Vol.3 No.10.

[5] Y. Wu, C. Hsiao, "Reliability Assessment of Automated Eddy Current System for Turbine Blade," NDT.net, Vol. 7, No. 11, November 2002.

[6] S. Burke, "Crack Depth Measurement using Eddy-Current NDE," 10th Asia-Pacific Conference on Non-Destructive Testing , 17-21 September 2001, Brisbane, Australia.

[7] D. Moore and F. Spencer, " Interlayer Crack Detection Results Using Sliding Probe Eddy Current Procedures," 10th Asia-Pacific Conference on Non-Destructive Testing , 17-21 September 2001, Brisbane, Australia.

[8] B. Wincheski, J. P. Fulton, S. Nath, M. Namkung, and J. W. Simpson, "Self-Nulling Eddy Current Probe for Surface and Subsurface Flaw Detection," in Materials Evaluation, Vol. 52/Number 1 (January 1994).

[9] Ryszard Sikora, Piotr Baniukiewicz, "The Complete Measurement System for Crack," Proceedings of the VIth International Workshop, Computational Problems of Electrical Engineering, Institute of Theory of Electrical Engineering, Zakopane, Poland, September 1-4, 2004.

[10] T.K. O'Brien and D.C. Kunerth, "Pulsed Eddy Current Thickness Measurements of Transuranic Waste Containers," US Dept of Energy, Report number INEL--95/00313; CONF-951091-12, 1995.

[11] J. Skramstad, R. Smith and David Harrison, "Enhanced detection of deep corrosion using transient eddy currents," Proc. 7th Joint DoD/FAA/NASA Conference on Aging Aircraft, New Orleans, Sept 2003.

[12] "Measuring Coating Thickness," CMI International Inc., Elk Grove Village, Illinois, http://www.pfonline.com/articles/pfd0027.html, accessed on November 7, 2005.

[13] A. Salem, T. Nayfeh, and C Fox, "Nondestructive Quality Assurance Testing of Chemically Processed Wood," Int. Journal Advanced Manufacturing Technology, Springer-Verlag London Limited, Vol. 26, pp. 1275-1283, January 2005.

[14] Yaron Danon, Changqing Lee, Chris Mulligan, and Greg Vigilante, "Characterizing Tantalum Sputtered Coatings on Steel by Using Eddy Currents," IEEE TRANSACTIONS ON MAGNETICS, VOL. 40, NO. 4, JULY 2004, pp. 1826-1832.

[15] Operating Manual, MIZ-21B Eddy Current System, Zetec, inc., 2003.

[16] Manymouse, http://www.icculus.org/manymouse/, visited July, 2006

[17] W. Jasper, "Linux Drivers", ftp://lx10.tx.ncsu.edu/pub/Linux/drivers/, visited July, 2006.

[18] OpenGL, http://www.opengl.org, visited July, 2000.